Available online at www.sciencedirect.com
ScienceDirect
Catalysis Today 117 (2006) 259–264
CATALYSIS TODAY
www.elsevier.com/locate/cattod

A new approach to the preparation of MoVNbTe mixed oxide catalysts for the oxidation of propane to acrylic acid

Xinlin Tu *, Naomasa Furuta, Yuuichi Sumida, Mamoru Takahashi, Hiroshi Niiduma

Macromolecular Research Laboratory, Toagosei, 455-0027 Nagoya, Japan

Available online 10 July 2006

Abstract

A new approach using fine metallic tellurium, such as tellurium fibers for Te source and adding porosity generation substances to the preparation of MoVNbTe mixed oxide catalyst aimed at selective oxidation of propane to acrylic acid has been developed. This approach leads to an enrichment of phase M1, the most effective phase for the reaction, of the phase constitution and provides uniform crystalline particles with a low level of agglomeration and a high surface area. The obtained catalyst exhibited a 48% acrylic acid yield (63.4% conversion and 75.6% selectivity) under a reaction temperature of 380 °C and a low steam/propane ratio of 6.5.

Keywords: Propane oxidation; Fine metallic tellurium; Tellurium fibers; Porous precursor

1. Introduction

The one-step selective oxidation of propane into acrylic acid has attracted widespread interest among researchers in both academic and industrial domains [1–32]. The most effective catalyst system for this reaction is the MoVNbTe mixed oxide catalyst, as first patented by Mitsubishi Chemicals [1,2]. A yield of 48.5% with 60.5% acrylic acid selectivity has been claimed under a reaction temperature of 380 °C and a steam/propane ratio of 14. The high steam ratio condition is crucial to obtain a high selectivity of acrylic acid, but is impractical due to the costs of downstream operations. Thus, a high performance by the catalyst while operating under a low steam/propane ratio is desirable for the industrial application of this catalyst system.

As another promising catalyst system for the same reaction, the authors revealed [8] independently with Mitsubishi Chemicals [3], the effectiveness of a MoVNbSb mixed catalyst using a slurry method. For this catalyst system, the adoption of a non-solution precursor through a heat treatment of a mixture of antimony trioxide, ammonium heptamolybdate and ammonium metavanadate [8,9] followed by adding an oxidant to the slurry or by a stepwise addition of ammonium heptamolybdate [8–11,22,29] provided optimal catalytic performance of catalyst. The non-solution precursor allows the existence of various species in different valence states (in a non-equilibrium state) and therefore provides a diversity of intermediates to fit the formation of active phase [29].

Comparing with the antimony-based system, tellurium-based catalysts have been prepared with a soluble precursor except for hydrothermal synthesis [4,5]. One motive of this study is therefore to investigate whether the non-solution approach used in the Sb-based system is applicable to tellurium-based catalysts and promotes their catalytic performance. For this purpose, a slurry method using fine metallic tellurium sources and adding substances to generate porosity has been designed and examined over the reaction of selective oxidation of propane to acrylic acid.

This paper describes the performance of the catalysts and discusses the role of each additive and the feature of the catalysts.

2. Experimental

2.1. Tellurium sources

Fine metallic tellurium was synthesized by the heat treatment of aqueous slurry composed of TeO_2 (MITSUWA PURE CHEMICALS, 99.9%), hydrazine hydrate (WACO Chemicals, 80 wt.%) as reducing agent and distilled water at 80 °C while stirring for 4 h followed by rinsing of the remaining hydrazine hydrate with distilled water [30]. For comparison, metallic tellurium (MITSUWA PURE CHEMICALS, 99.9%),

* Corresponding author. Tel: 81 52 611 9916; fax: 81 52 614 0270
E-mail address: shinrin_to@mail.toagosei.co.jp (X. Tu).

0920-5861/$ – see front matter © 2006 Elsevier B.V. All rights reserved.
doi:10.1016/j.cattod.2006.05.059

ball-mill ground metallic tellurium and telluric acid (MITSUWA PURE CHEMICALS, 99.9%) were also used in the preparation of catalysts.

2.2. Catalyst preparation

The MoVTeNbO catalysts, using fine metallic tellurium and other metallic tellurium sources, were prepared following a slurry method [30]. An aqueous solution of ammonium heptamolybdate (WAKO CHEMICALS, 99%), ammonium metavanadate (WAKO CHEMICALS, 99%) and an aqueous suspension of tellurium source were mixed and heated for the required time, depending on the tellurium sources as described below. Blue slurry was formed following the oxidation and reduction reactions among the Te, Mo and V sources. Co-precipitation between an aqueous solution of niobium oxalate, prepared by heating an aqueous slurry of $Nb_2O_5{\cdot}xH_2O$ (CBMM, assay 80%) and oxalic acid (WACO Chemicals, 99.9 wt.%) with a molar ratio of oxalic acid to Nb 3.5, and the above blue slurry was found to occur when they were mixed by stirring. Ammonium nitrate with a molar ratio of NH_4NO_3 to Mo 0.37 was added to samples Cat A, B, C, respectively, after mixing the niobium oxalate solution with the slurry of the Mo, V, and Te sources. For samples from Cat 1 to 10, an aqueous ammonia and ammonium nitrate were added in amounts described in Table 1, respectively, before and after mixing the niobium oxalate solution with the slurry of the Mo, V, and Te sources.

The slurry obtained was then evaporated to dryness at 120 °C for 3 h followed by a pre-calcination at a temperature under 300 °C for 1.5 h in a crucible and calcination under 590 °C for 1 h within a stainless steel tube which was sealed with small amount of quartz wool and active carbon.

The MoVTeNbO catalysts using telluric acid (Cat 11) were prepared according to Ref. [2].

2.3. Catalyst characterization

SEM images were measured with a JEOL JSM-6330F field emission scanning electron microscope. The powder X-ray diffraction (XRD) was measured via a continuous scanning (3°/min) method; using a Rigaku RINT 2000 automatic diffractometer with Cu K_α radiation. Metallic Fe, which showed a major diffraction peak with 2θ at 44.7°, was added as a reference substance to evaluate the crystallinity of the catalyst. The BET surface area was determined with a HORIBA SA-6200 Series unit, while elemental analysis was performed through a wave dispersive XRF using a Rigaku ZSM 100e instrument.

2.4. Catalyst evaluation

The catalyst evaluations were performed using a fixed bed quartz tubular reactor (i.d. 8 mm). The catalysts, once pelletted and crushed into granules of 15–30 mesh, were packed into the reactor for evaluation. The reactions were carried out under 1 atm of pressure, a reaction temperature of 380 °C, and a feed mixture with a molar ratio of propane/air/steam = 1/9.0/6.5 and a SV of 2400 h^{-1}. Reactants and products were analyzed using gas chromatography. The conversion, selectivity and yield expressed in molar percentage form were calculated on a propane base.

3. Results and discussion

3.1. Effect of variety of tellurium sources

Fig. 1 shows SEM image of the tellurium sources used in the preparation of catalysts. The metallic tellurium used is composed of agglomerates with size-distribution from 5 to 20 μm. Ball-mill grinding in the presence of hydrogen peroxide (H_2O_2/Te = 0.7) crushed the agglomerates to their primary particle size of 0.5–2.0 μm. On the other hand, the reduction of TeO_2 with hydrazine hydrate (hydrazine/Te = 2.0) revealed a fiber-like shape with a uniform section diameter of ca. 100 nm, and lengths from 400 to 1000 nm.

Fig. 2 shows the XRD patterns of the as-dried (at 50 °C) samples corresponding to Fig. 1. All the samples showed a set of diffraction lines with 2θ at 23.0°, 27.6°, 38.3°, 40.4°, 43.3°, 45.9°, 49.6° which are consistent with hexagonal tellurium

Table 1
Effect of amount of additives on the catalytic performance of catalysts[a]

Sample	Additives (mol ratio) (NH_4OH/NH_4NO_3/Mo)	Propane conversion (%)	AA selectivity (%)	XRD index				S_{BET} (m^2/g)	Average valence state number[b]
				$I_{27.2°}$[c]	$I_{28.2°}$[c]	$I_{27.2°}/I_{28.2°}$	$I_{22.2°}/I_{Fe}$[d]		
1	0/0/1	15.1	71.0	24	31	0.77	1.32	7.0	4.73
2	0.3/0.3/1	28.9	69.3	25	26	0.96	1.55	10.1	4.56
3	0.41/0.41/1	52.8	74.0	33	24	1.38	1.92	17.5	4.86
4	0.41/0.52/1	58.1	76.2	33	18	1.83	1.87	14.6	4.92
5	0.52/0.41/1	57.3	76.3	33	20	1.65	1.64	14.8	4.99
6	0.46/0.46/1	57.2	77.2	33	20	1.65	1.85	17.3	5.05
7	0.52/0.52/1	63.4	75.6	36	18	2.00	1.79	14.6	4.96
8	0.58/0.58/1	61.4	73.7	35	17	2.06	2.00	15.0	4.95
9	0.64/0.64/1	59.6	65.9	39	24	1.63	1.79	19.6	4.99
10	0.7/0.7/1	53.0	58.5	32	22	1.45	2.08	19.5	4.92

[a] All the catalyst compositions are $MoV_{0.26}Te_{0.14}Nb_{0.16}$ as determined by XRF.
[b] Represent the average valence state number of Mo, V, Nb, and Te calculated from the elemental composition determined by XRF.
[c] The relative intensities with respect to the diffraction line of 22.1°.
[d] Using the diffraction peak of metallic Fe with 2θ at 44.7°.

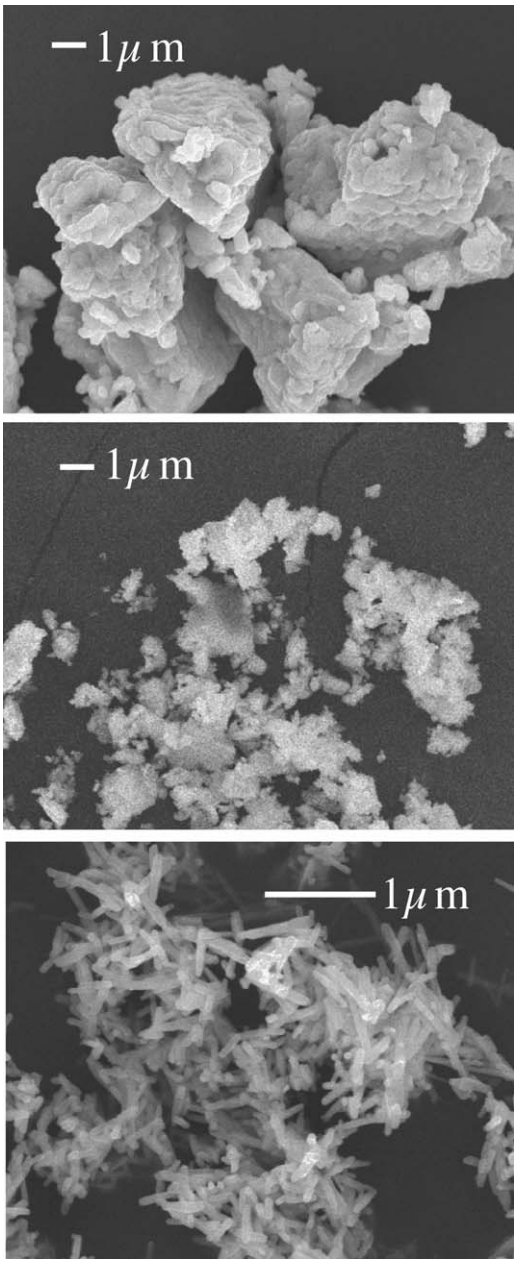

Fig. 1. SEM image of metallic tellurium (top), ground metallic tellurium (middle) and reduced tellurium (bottom) used for preparation of catalysts.

(JCPDS 36-1452). Minor diffraction lines with 2θ at 26.2°, 29.9°, 48.6°, due to TeO_2 impurity (JCPDS 42-1365) were observed on samples derived from metallic tellurium. No obvious diffraction lines owing to TeO_2 phases were detected for reduced tellurium indicating that the reduction of TeO_2 had totally occurred.

Fig. 3 shows the XRD patterns of the as-dried catalyst prepared with different tellurium sources. The patterns indicate basically an amorphous property of the samples at this stage. A weak diffraction line with 2θ at 27.6° assigned to hexagonal tellurium can be seen for all the samples indicating that tellurium source partly remained as crystalline phase even after drying at 120 °C for 3 h. Other minor impurity phases with 2θ at 8.2° and 29.1° in the case of metallic tellurium and ground tellurium are most likely due to hydrates of Mo and V compound.

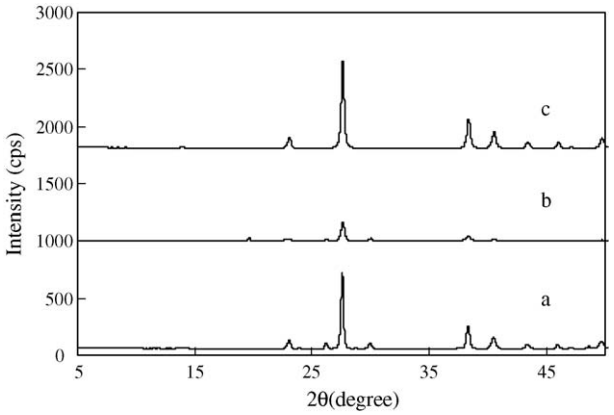

Fig. 2. XRD patterns of tellurium sources corresponding to Fig. 1. (a) Metallic tellurium; (b) ground tellurium; (c) reduced tellurium.

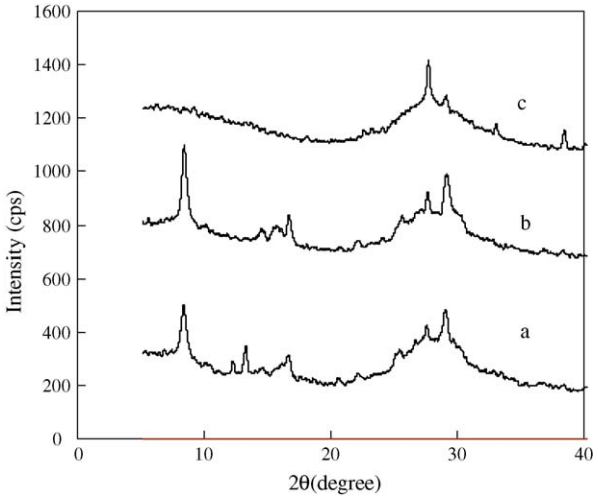

Fig. 3. XRD patterns of the as-dried catalysts prepared with different tellurium sources corresponding to Fig. 1. (a) Catalyst prepared with metallic tellurium; (b) catalyst prepared with ground tellurium; (c) catalyst prepared with reduced tellurium.

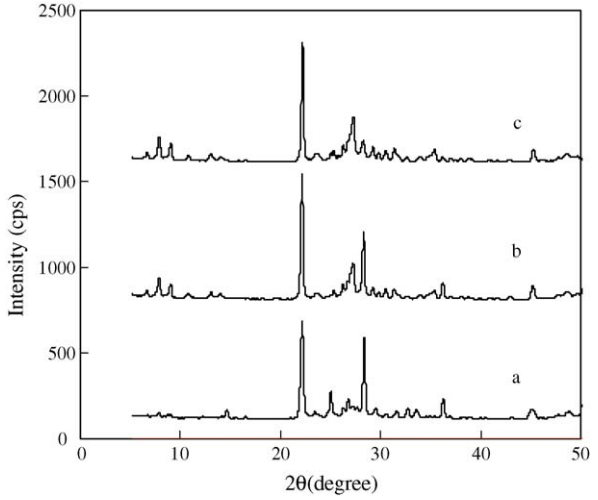

Fig. 4. XRD patterns of the as-calcined catalysts prepared with tellurium sources corresponding to Fig. 1. (a) Catalyst prepared with metallic tellurium; (b) catalyst prepared with ground tellurium; (c) catalyst prepared with reduced tellurium.

Table 2
Catalytic performance of catalysts prepared with different tellurium sources[a,b]

Catalyst number	Te source	Additive (mol ratio) (NH_4NO_3/Mo)	Propane conversion (%)	Selectivity (%)				AA yield (%)
				AA	ACA	PP	COx	
Cat A	Metallic Te	0.37	16.2	23.2	17.2	3.1	56.5	3.8
Cat B	Ground Te	0.37	36.4	65.7	11.1	2.2	21	23.9
Cat C	Reduced Te	0.37	48.5	76.2	6.5	1.4	15.9	37.0

[a] Catalyst composition (as determined by XRF measurement): $MoTe_{0.18}V_{0.26}Nb_{0.18}$.
[b] Heat treatment time of Te with Mo, V components: Cat A, 12 h; Cat B, 1 h; Cat C, without heat treatment.

Fig. 4 shows the XRD patterns of the as-calcined catalysts. All the catalysts showed major diffraction lines with 2θ at 22.1°, 26.1°, 26.6°, 28.2° assigned to a hexagonal phase M2, and 2θ at 6.6°, 7.8°, 22.2°, 27.2° assigned to an orthorhombic phase M1 [2,17,18,24]. The ratios of phase M1 to phase M2 as expressed by the ratio of intensity of line with 2θ at 27.2° to that at 28° varied depending on the tellurium source. The ratio is 0.06 for that prepared with metallic tellurium, increasing to 0.35 and 1.73 for that with ball-mill ground and reduced tellurium, respectively. The catalyst prepared with metallic tellurium showed extra diffraction peaks with 2θ at 14.0°, 24.9° which is assigned to the MoO_3 phase (JCPDS 5-508); indicating phase separation of Mo with the Nb component. The catalyst with ball-mill ground tellurium and tellurium reduced from TeO_2 showed almost no diffraction lines due to this phase.

The performance of the catalysts was summarized in Table 2. In the case involving use of the metallic tellurium source, the performance depended on the duration of heat treatment of metallic tellurium with Mo and V sources. The optimal heating time was 12 h, but the yield of acrylic acid was as low as 3.8%. Ball-mill grinding of metallic tellurium shortened the time to one hour and increased the yield to 23.9%, while the catalyst with reduced tellurium exhibited a 37% yield without heat treatment. These results indicate a positive effect of a small tellurium particle size and certain negative effects of reactions among Mo, V, Te sources. During the heat treatment process, the occurrence of oxidation and reduction reactions among Te, Mo^{6+} and V^{5+} species trigger the dispersion of tellurium and the formation of a blue slurry; containing reductive Mo compound generally called molybdenum blue [35]. The dispersion of tellurium is desirable, while the presence of molybdenum blue, which tends to condense into large polyoxometalates [35], is unfavorable for the incorporation of Nb *via* precipitation. The XRD data for the presence of the MoO_3 phase when using metallic tellurium supported the above assumption. By comparing the XRD pattern and performance of these catalysts, the performance of the catalyst can be seen to be closely connected with the ratio of M1 to M2; suggesting that fine metallic tellurium improves catalytic performance by enhancing the formation of phase M1.

3.2. Effect of the addition of ammonium nitrate and aqueous ammonia

By optimizing parameters for the preparation of the catalyst, a further improvement in catalytic performance was obtained. Among them, an increase in the amount of ammonium nitrate combined with the addition of aqueous ammonia and adjustment of the elemental composition were found to be most effective. The catalytic performance and change in the physicochemical properties were summarized in Table 1. A 48% yield with 76% selectivity of acrylic acid was obtained under optimal conditions. These included the addition of ammonium nitrate and aqueous ammonia in a molar ratio of 0.52 to Mo component, the addition of aqueous ammonia before the Mo, V, Te slurry was mixed with niobium oxalate and using an elemental composition of $MoV_{0.26}Te_{0.14}Nb_{0.16}O_{3.87}$.

As shown in Table 1, with the change of the amount of ammonium nitrate and aqueous ammonia, the BET. specific surface area, the ratio of XRD peak intensity of 27.2–28.2° of 2θ, the crystallinity in term of the relative diffraction intensity of 22.2° of 2θ to that of reference substance of Fe (44.7° of 2θ), and the average valence state number of Mo, V, Te and Nb components varied suggesting a very complicated phenomenon.

To understand the relationship between the physicochemical properties and the catalytic performance of the catalyst, correlations between them were examined. As shown in Fig. 5, excellent linear relationships between the conversion of

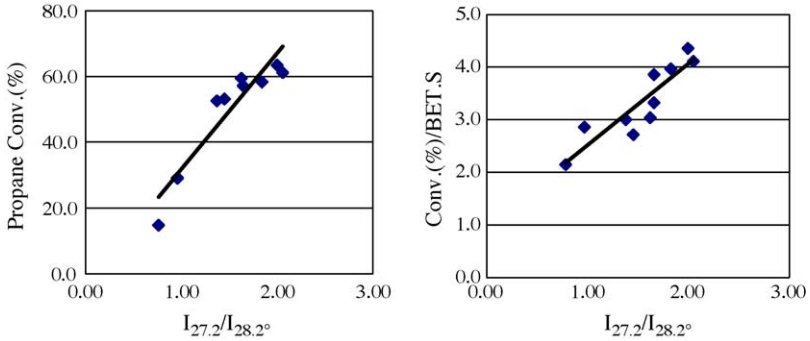

Fig. 5. Correlation of the conversion of propane, conversion per BET surface area to the ratio of XRD peak intensity corresponding to data shown in Table 1.

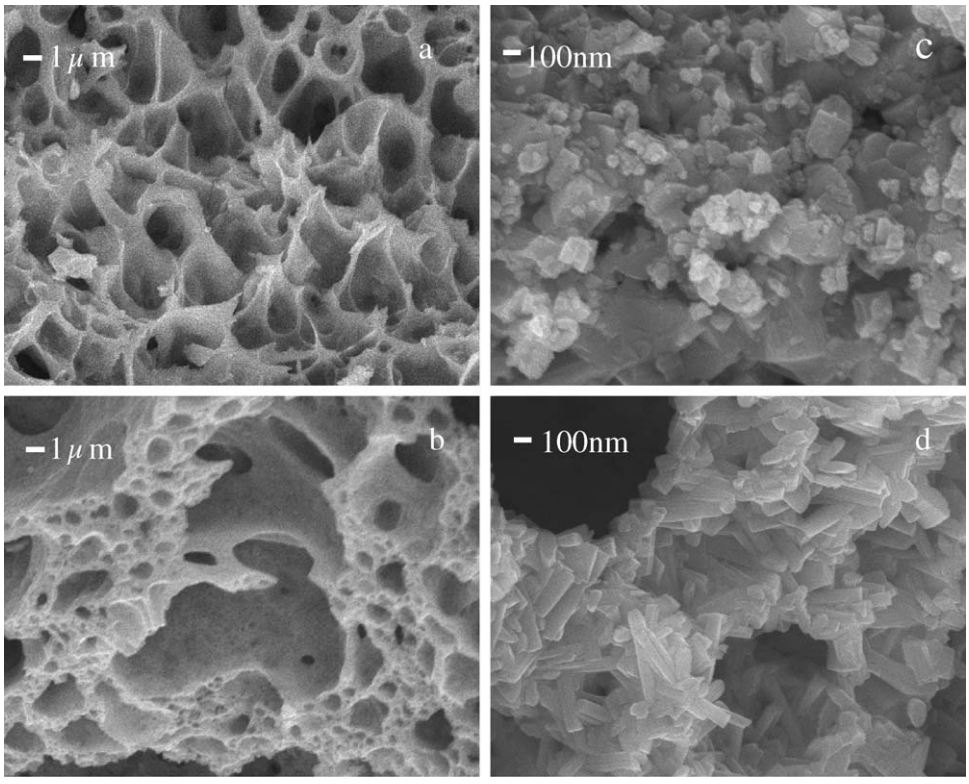

Fig. 6. SEM image of the as-precalcined and as-calcined catalysts prepared with and without the addition of ammonium nitrate and aqueous ammonia. The as-precalcined catalysts with (b) and without (a) the addition of ammonium nitrate and aqueous ammonia. The as-calcined catalysts with (d) and without (c) the addition of ammonium nitrate and aqueous ammonia.

propane and the ratio of XRD peak intensity of 27.2–28.2° of 2θ, the conversion of propane per BET. specific surface area and the ratio of XRD peak intensity of 27.2–28.2° of 2θ were obtained indicating a dominating and independent effect of phase constitution and a positive effect of surface area on the performance of catalyst. On the other hand, relatively poor correlations of conversion to other properties suggest their indirect relationship with the activity.

Fig. 6 shows SEM images of the as-precalcinated and as-calcined catalysts prepared with and without the addition of ammonium nitrate and aqueous ammonia, respectively. Without the addition, although the precursor contains some pore structure, it is a dense solid on the whole. Corresponding to the precursor, the as-calcined catalyst exhibited an irregular shape and a particles subject to considerable agglomeration. The addition of ammonium nitrate and aqueous ammonia prompted the appearance of small submicroscopic pores, generating the continously porous texture of the precursor. Ammonium nitrate is known to undergo explosive decomposition due to inner-molecular reactions at temperatures exceeding 260 °C. Therefore, in this case, Ammonium nitrate possibly undergoes a rapid decomposition leading to the porous texture of the precursor. The porosity inhibits the sintering of the formed crystalline leading to a low extent of agglomeration and a relatively high surface area. As for the effect of the aqueous ammonia, it prabobly neutralizes the oxalic acid in slurry and thus prevent the ammonium nitrate from hydrolysis.

The manner by which ammonium nitrate and aqueous ammonia affect the phase constitution, however, remains unclear. One assumption is that the porous texture over a large surface area of the precursor, generated by the addition of

Table 3
Performance of catalysts prepared with fine metallic tellurium and telluric acid

Sample number	Te source	Additives (mol ratio) (NH_4OH/NH_4NO_3/Mo)	Propane conversion (%)	AA selectivity (%)	XRD index ($I_{27.2°}/I_{28.2°}$)	S_{BET} (m^2/g)	Average valence state number[a]
11	Telluric acid[b]	0/0/1	34.2	64.5	0.11	7.0	5.43
12	Telluric acid[b]	0/0.37/1	16.2	65.9	0.12	6.8	5.57
13	Telluric acid[c]	0.52/0.52/1	13.3	69.4	1.35	8.7	5.77
7	Reduced Te[c]	0.52/0.52/1	63.4	75.6	2.00	14.6	4.96

[a] Average valence state number of Mo, V, Nb, and Te calculated from the elemental composition.
[b] The elemental compositions are $MoV_{0.30}Te_{0.23}Nb_{0.12}$ as determined by XRF.
[c] The elemental compositions are $MoV_{0.26}Te_{0.14}Nb_{0.18}$ as determined by XRF.

ammonium nitrate, may affect the crystallization process by increasing diffusion resistance. Since phase M2 crystallizes more slowly than M1 [34], the diffusion resistance may favor the formation of phase M1.

3.3. The comparison of catalysts prepared with telluric acid and fine metallic tellurium

Table 3 summarizes the catalytic performance and some physicochemical properties of catalysts prepared with telluric acid and fine metallic tellurium (reduced tellurium). Those prepared with telluric acid gave a 22.1% yield of acrylic acid, lower than a half of that using the reduced tellurium. Adding ammonium nitrate and aqueous ammonia and adjustment of the elemental composition did not improve the catalytic performance. Therefore, the above results indicate that the non-solution approach; using fine metallic tellurium combined with the addition of ammonium nitrate and aqueous ammonia, is superior to that using soluble telluric acid.

The above result appears contradictory to the general principle of the necessity of homogeneity for the catalyst precursor. However, the low melting point of metallic tellurium (near 460 °C) and a high vapor pressure of TeO_2 are unique. It is known that atoms or ions are mobile for bulk-to-surface migration when the temperature is raised to Tammann temperature (ca. half the melting point) [36]. Thus a diffusion process of the tellurium species accompanying the solid state reactions in oxidation and reduction mode among the Mo, V and Te species possibly occurs before and/or during the precalcined steps at 300 °C. The sublimation of the tellurium species at calcination step under a temperature of 590 °C will aid its incorporation into the cryastalline phase of catalysts.

In addition, one drawback concerning the use of soluble telluric acid for the preparation of the catalyst has been pointed out. Oliver et al. reported that telluric acid tends to form an Anderson type molybdotellurate with Mo source at a PH of above 4.5, which negatively affects performance [33]. The low solubility of metallic tellurium probably minimizes the formation of impurities between the tellurium and Mo components and favors the incorporation of the niobium component. This assumption is consistent with the high ratio of Nb to Te of the optimal catalyst using fine metallic tellurium comparing with that using telluric acid. Although the details remain under investigation, the non-solution property of precursors derived from fine metallic tellurium would be important for the catalytic performance.

4. Conclusion

This work demonstrated the effectiveness of a non-solution precursor prepared with fine metallic tellurium for the preparation of MoVNbTe mixed oxide catalyst aimed at the selective oxidation of propane to acrylic acid. The combined use of fine metallic tellurium with the addition of porosity generating substances such as ammonium nitrate and aqueous ammonia allows the enrichment of the orthorhombic phase M1 on a fixed elemental composition of mixed oxide. It also provides uniform particles of crystalline with a low level of agglomeration and a high surface area. The mixed oxide catalyst obtained exhibited a 48% acrylic acid yield (63.4% conversion and 75.6% selectivity) under a reaction temperature of 380 °C and a low steam/propane ratio of 6.5.

Acknowledgements

Thanks are given to Tadashi Hattori, Professor Emeritus of Nagoya University and Atsushi Satsuma, Professors of Nagoya University for their fruitful discussions and helpful advice during the work.

References

[1] T. Ushikubo, H. Nakamura, JP Patent 94,279351 (1994).
[2] T. Ushikubo, Y. Koyasu, S. Wajiki, JP Patent 95,10801 (1995).
[3] T. Ushikubo, Y. Koyasu, H. Nakamura, JP Patent 98,45664 (1998).
[4] W. Ueda, K. Oshihara, Appl. Catal. A 200 (2000) 135.
[5] W. Ueda, Catal. Today 71 (2001) 1.
[6] M. Lin, T.B. Desai, F.W. Kaiser, P.D. Klugherz, Catal. Today 61 (2000) 223.
[7] M.M. Lin, Appl. Catal. A 207 (2001) 1.
[8] X. Tu, M. Takahashi, M. Ishii, JP Patent 97,316,023 (1997).
[9] X. Tu, M. Takahashi, S. Hirose, JP Patent 98,137585 (1998).
[10] X. Tu, M. Takahashi, S. Hirose, JP Patent 98,230164 (1998).
[11] M. Takahashi, X. Tu, S. Hirose, JP Patent 99,285,636 (1999).
[13] H. Watanabe, Y. Koyasu, Appl. Catal. A 194 (2000) 479.
[14] T. Ushikubo, Catal. Today 57 (2000) 331.
[15] T. Shishido, T. Konishi, I. Matsuura, Y. Wang, K. Takaki, K. Takehira, Catal. Today 71 (2001) 77.
[16] S.A. Holmes, J. Al-Saeedi, V.V. Guliants, P. Boolchand, D. Georgiev, U. Hackler, E. Sobkow, Catal. Today 67 (2001) 403.
[17] M. Aouine, J.L. Dubois, J.M.M. Millet, Chem. Commun. 13 (2001) 1180.
[18] J.M.M. Millet, H. Roussel, A. Pigamo, J.L. Dubois, J.C. Jumas, Appl. Catal. A 232 (2002) 77;
J.N. Al-Saeedi, V.V. Guliants, Appl. Catal. A 237 (2002) 111.
[19] E.K. Novakova, J.C. Vedrine, E.G. Derouane, J. Catal. 211 (2002) 226.
[20] H. Tsuji, Y. Koyasu, J. Am. Chem. Soc. 124 (2002) 5608.
[21] T. Ushikubo, Catal. Today 78 (2003) 79.
[22] X. Tu, M. Takahashi, H. Niiduma, JP Patent 2003,103168 (2003).
[23] M. Baca, A. Pigamo, J.L. Dubois, J.M.M. Millet, Top. Catal. 23 (2003) 39.
[24] P. DeSanto Jr., D.J. Buttrey, R.K. Grasselli, C.G. Lugmair, A.F. Volpe, B.H. Toby, T. Vogt, Top. Catal. 23 (2003) 23.
[25] R.K. Grasselli, J.D. Burrington, D.J. Buttrey, P. DeSanto Jr., C.G. Lugmair, A.F. Volpe, T. Weingand, Top. Catal. 23 (2003) 5.
[26] R.K. Grasselli, D.J. Buttrey, P. Desanto Jr., J.D. Burrington, C.G. Lugmair, A.F. Volpe Jr., T. Weingand, Catal. Today 91/92 (2004) 251.
[27] M.M. Lin, Appl. Catal. A 250 (2003) 287.
[28] M. Baca, A. Pigmo, J.L. Dubois, J.M.M. Millet, Top. Catal. 23 (2003) 39.
[29] X. Tu, N. Hashimoto, Y. Sumita, H. Niiduma, JP Patent 2004,41880 (2004).
[30] X. Tu, Y. Sumita, M. Takahashi, H. Niiduma, WO 091779 A1 (2004).
[31] T. Kato, D. Vitry, W. Ueda, Catal. Today 91/92 (2004) 237.
[32] W. Ueda, D. Vitry, T. Kato, Catal. Today 96 (2004) 235.
[33] J.M. Oliver, J.M. Lopez Nieto, P. Botella, A. Mifsud, Appl. Catal. A 257 (2004) 67.
[34] Unpublished data of the authors.
[35] A. Muller, J. Meyer, E. Krickemerer, W. Diemann, Angew. Chem. Ed. Engl. 30 (1996) 1206.
[36] P.G. Menon, B. Delmon, in: G. Ertl, H. Knozinger, J. Weitkamp (Eds.), Handbook of Heterogenous Catalysis, Wiley-VCH, New York, 1997 , p. 104 (Chapter 2.1.6).